International Journal of Biological Macromolecules 252 (2023) 126060

Contents lists available at ScienceDirect

International Journal of Biological Macromolecules

journal homepage: www.elsevier.com/locate/ijbiomac

An injectable photopolymerizable chitosan hydrogel doped anti-inflammatory peptide for long-lasting periodontal pocket delivery and periodontitis therapy

Zihe Hu [1], Yanyan Zhou [1], Haiyan Wu, Gaoying Hong, Mumian Chen, Wenjing Jin, Weiying Lu, Minghao Zuo, Zhijian Xie [*], Jue Shi [*]

Stomatology Hospital, School of Stomatology, Zhejiang University School of Medicine, Zhejiang Provincial Clinical Research Center for Oral Diseases, Key Laboratory of Oral Biomedical Research of Zhejiang Province, Cancer Center of Zhejiang University, Engineering Research Center of Oral Biomaterials and Devices of Zhejiang Province, Hangzhou 310000, China

ARTICLE INFO

Keywords:
Injectable
Hydrogel
Periodontitis
Anti-inflammation
Periodontal preservation

ABSTRACT

Periodontitis is a common chronic inflammatory disease caused by plaque that leads to alveolar bone resorption and tooth loss. Inflammation control and achieving better tissue repair are the key to periodontitis treatment. In this study, human β-Defensin 1 short motif Pep-B with inflammation inhibition and differentiation regulation properties, is firstly used in the treatment of periodontitis, and an injectable photopolymerizable Pep-B/chitosan methacryloyl composite hydrogel (CMSA/Pep-B) is constructed. We confirm that Pep-B improves inflammation, and restores osteogenic behavior and function of injured stem cells. CMSA/Pep-B has good injectability, fluidity and photopolymerizability, and can sustainably release Pep-B to maintain drug concentration in periodontal pockets. Furthermore, animal experiments showed that CMSA/Pep-B significantly ameliorated the inflammation of the periodontium and reduced the alveolar bone loss by decreasing inflammatory infiltration, osteoclast formation and collagen destruction. In conclusion, CMSA/Pep-B is envisaged to be a novel bioactive material or therapeutic drug for treating periodontitis.

1. Introduction

Periodontitis is a chronic inflammatory disease of polymicrobial etiology which can cause inflammatory periodontal bone tissue resorption [1]. It may even result in tooth loss if left untreated, severely compromising the patient's quality of life [2,3]. Furthermore, it has been reported to be closely related to certain systemic diseases like chronic kidney disease, cardiovascular disease and diabetes [4,5]. Studies have demonstrated that treatment of periodontitis can promote recovery of systemic diseases, which further signifies its economic and medical merit [6,7]. The inflammatory microenvironment plays an important role in regulating the development of periodontal disease, and multiple inflammatory stimuli can cause irreversible destruction of periodontal tissues, such as alveolar bone loss and gingival recession [8]. Therefore, exploring novel therapeutics that can control inflammation and reduce periodontal tissue destruction in an inflammatory microenvironment of periodontitis is gaining immense attention.

The traditional treatment modality for periodontitis includes the use of antibacterials, but they face shortcomings of limited effectiveness and microbial resistance [9,10]; their use can cause the release of several bacterial byproducts such as LPS and phosphatidic acid, further exacerbating the local inflammatory response [11]. In addition, systemic delivery required substantial doses of medications to reach the minimum therapeutic concentration, which may result in unfavorable consequences such as toxicity and gastrointestinal intolerance [12]. In contrast, local treatment can deliver high drug concentrations with minimal side effects, improving efficacy and patient compliance [13]. Therefore, there is an urgent clinical need to create innovative local application materials with excellent security and efficiency to reduce inflammation and protect damaged periodontal tissue.

* Corresponding authors.
E-mail addresses: huzihe@zju.edu.cn (Z. Hu), ss.yanyanzhou@zju.edu.cn (Y. Zhou), 3160103741@zju.edu.cn (H. Wu), gaoying_h@zju.edu.cn (G. Hong), 3180102597@zju.edu.cn (M. Chen), wjjin@zju.edu.cn (W. Jin), 22118772@zju.edu.cn (W. Lu), 22118732@zju.edu.cn (M. Zuo), xzj66@zju.edu.cn (Z. Xie), dentistsj@zju.edu.cn (J. Shi).
[1] Equal contribution

https://doi.org/10.1016/j.ijbiomac.2023.126060
Received 15 March 2023; Received in revised form 27 July 2023; Accepted 28 July 2023
Available online 29 July 2023
0141-8130/© 2023 Published by Elsevier B.V.

Due to the irregular anatomical structure of the periodontal pocket, injection is a common mode of drug administration for periodontitis treatment. [14] The drug-loaded carrier is noninvasively injected into the periodontal pocket, where it continuously releases the drug locally. The administration method can increase patient comfort and improves drug bioavailability. Chitosan methacryloyl (CMSA) is a reliable biocompatible, biodegradable, controlled-release material [15,16]. The CMSA can repair irregularly shaped tissue defects with a simple injection of a pre-gel solution, which can then be photocrosslinked with UV light to form a matrix system continuously releasing the drug over an extended period [17,18], which advocates its merit to be used as a drug carrier for treating periodontitis.

Human defensin 1 (HBD1) is an endogenous cationic antimicrobial peptide with high activity against Gram-negative bacteria [19,20]. It also plays a role in innate-immune defense in disease states, such as immune response and inflammation regulation. [21,22]. Pep-B is a functional fragment of HBD1 with antibacterial activity comparable to the full-length HBD1 protein [23]. Its small molecular weight enables quick and easy synthesis and can thus be modified and optimized, which makes it an ideal candidate to accelerate its clinical transformation and applicability. Furthermore, our previous studies have verified that Pep-B could reduce the inflammatory response and restore osteogenic differentiation of stem cells in an inflammatory state [24]. As a result, Pep-B is a promising candidate to be used an adjuvant/alternative to antibiotics in the treatment of periodontitis.

Herein, we developed a CMSA/Pep-B hydrogel loaded Pep-B that was injectable and photopolymerizable under UV light and could sustainably release Pep—B. The Pep-B holds anti-inflammatory potential and can rescue the osteogenic differentiation of periodontal ligament stem cells (PDLSCs). In addition, we demonstrated that the CMSA/Pep-B hydrogel could ameliorate periodontal inflammation and promote alveolar bone regeneration in rat periodontitis models.

2. Materials and methods

2.1. Materials and reagents

Peptides, primers sequences (Sangon, China). DMEM medium, Penicillin/Streptomycin, fetal bovine serum (Gibco, California). Trypsin, LPS, dexamethasone, β-sodium glycerophosphate, ascorbic acid, alizarin red, cetylpyridinium chloride (Sigma Aldrich, St. Louis, Missouri). CCK8 assay kit, NO assay kit, lactate dehydrogenase (LDH) release assay kit, ROS assay kit, BCA protein assay kit, RIPA lysis, protease inhibitor, BCIP/NBT alkaline phosphatase color development Kit, alkaline phosphatase assay kit (Beyotime, China). Antibodies of CD29, CD45, CD34, CD90, CD105, CD11b (Biolengend, USA); antibodies of β-actin, inducible nitric oxide synthase (iNOS), interleukin-6 (IL-6) and IL-1β (Cell Signaling Technology, USA). TRIzol (Invitrogen, USA). DNA synthesis kit, SYBR Green System (TAKARA, Japan). ECL Kit (NCM biotech, China). Chitosan methacryloyl (CMSA), lithium phenyl (2,4,6-trimethylbenzoyl) phosphinate (Engineering For Life, China). All chemicals and reagents were purchased commercially and used without further purification.

2.2. Characters of Pep-B

Peptides were synthesized commercially by Sangon Biotech Co., Ltd. (Shanghai, China). The final chimeric sequence purity of Pep-B was examined by high performance liquid chromatography (HPLC, SHIMADZU, Japan). Pep-B molecular weight was determined using mass spectrometry (AB SCIEX, Framingham, USA). Raman spectroscopy (Renishaw, UK) and Circular Dichroism (CD, JASCO, Japan) spectrometer were used to investigate secondary structure of Pep—B. The lyophilized peptides were stored at −80 °C and dissolved in sterile water when used.

2.3. Cells isolation, culture and identification

With informed consent from the donors, the study samples were collected from the third molar teeth of healthy patients (18–25 years old), which were performed with the approval of the Ethics Committee of Zhejiang Stomatology Hospital. PDLSCs were isolated and cultured using the protocol previously reported [25]. The surface markers of PDLSCs were evaluated by flow cytometry. In brief, PDLSCs were digested with 0.25 % trypsin and incubated with following indicators for 30 min: anti-CD34-PE, anti-CD45-PE, anti-CD29-PE, anti-CD90-PE, anti-CD105-PE, and anti-CD11b-FITC. The fluorescence intensity and positive rate of the stained cells were analyzed with flow cytometry (BD bioscience Pharmingen, CytoFLEX LX, USA).

2.4. The effect of Pep-B on cytotoxicity and oxidative stress in LPS-stimulated cells

CCK8, lactate dehydrogenase (LDH), reactive oxygen species (ROS) and Griess assay were performed to evaluate the effect of Pep-B in LPS-stimulated PDLSCs. Briefly, cells were treated with 1 μg/ml LPS in the presence or absence of different concentrations of Pep-B for 24 h, then CCK-8 reagent, LDH assay kit, DCFH-DA and nitric oxide (NO) assay kit were performed according to the manufacturer's instructions to assess cytotoxicity and oxidative stress in different groups of PDLSCs.

2.5. Anti-inflammation effect of Pep-B

To evaluate the capability of Pep-B in countering inflammation, PDLSCs were exposed to 1 μg/mL LPS for 24 h with/without different concentrations of Pep—B, then Quantitative real-time polymerase chain reaction (RT-PCR) was performed to determine inflammation-associated mRNA levels. Briefly, TRIzol was used to extract total RNA and 500 ng RNA was converted to cDNA using the transcriptor first-strand complementary DNA synthesis kit. The RT-PCR was carried out with a SYBR Green System. Target gene expressions were normalized with GAPDH. The primers sequences are listed in Table S1.

2.6. The effect of Pep-B in osteogenic differentiation of LPS-stimulated PDLSCs

To detect the ability of Pep-B to ameliorate differentiation of LPS-stimulated PDLSCs, PDLSCs (1×10^5 cells/well) were cultured with osteogenic differentiation medium (containing 10 % FBS, 50 μg/ml ascorbic acid, 10 mmol/L β-glycerophosphate, 10 nmol/L dexamethasone) and treated with LPS in the presence or absence of different concentrations of Pep—B. The cells cultured with only differentiation medium were as control group. The medium was replaced after every two days.

2.6.1. Alkaline phosphatase (ALP) analysis

PDLSCs were first fixed with 4 % paraformaldehyde after 14 days of incubation, BCIP/NBT alkaline phosphatase colorimetry kit was performed to stain cells according to the manufacturer's instructions, and photos were taken using a digital camera. For quantitative ALP analysis, cells were lysed, the ALP content was measured by an Alkaline Phosphatase Assay Kit and normalized to the total protein content determined by a BCA protein assay kit.

2.6.2. Alizarin red staining (ARS)

Mineralized nodule formation was examined by 2 % Alizarin red staining (pH = 4.2) after osteoblast differentiation for 21 days. The mineral deposition was then dissolved using 10 % cetylpyridinium chloride to quantify alizarin staining, and optical densities (OD) values were measured at 562 nm using a microplate reader.

2.6.3. RT-PCR

After cultured for 7 and 14 days, the gene expression of osteogenic-related factors such as ALP, collagen type I (COL I), bone morphogenetic protein 2 (BMP2), and osteopontin (OPN) were detected using the procedure as mentioned in Section 2.5. The primers sequences are listed in Table S1.

2.7. Preparation of CMSA/Pep-B and characteristics

For formulating CSMA/Pep-B loaded hydrogels, CSMA was dissolved in double distilled water (ddH_2O) containing LAP (0.25 % *w/v*) at 60 °C under continuous magnetic stirring for 6 h in the dark. After that, the Pep-B solution was added under continuous magnetic stirring for another 4 h under ambient conditions. The CMSA/Pep-B solution was then sterilized employing a filtration using a 0.22 μm membrane filter. The morphology of the resulting hydrogels was observed by scanning electron microscope (SEM).

The rheological attributes of CMSA/Pep-B hydrogels, like storage modulus (G') and loss modulus (G"), were measured using a rheometer (TA, Discovery, USA) at a frequency of 50 Hz and 5 rad/s angular velocity under ambient conditions. UV light was used to irradiate the hydrogel through a gap after stable operation of the rheometer.

The Pep-B release rate from hydrogels was studied using a membrane-less protocol described previously [26]. In brief, samples of hydrogels (0.3 ml) were injected into the bottom of glass vials and then polymerized under UV light for 15 s. Subsequently, 2 mL of ddH_2O was gently added onto the surface of the hydrogels, and all samples were incubated at 37 °C with continuous gentle shaking. To measure the release of Pep—B, releasing medium were withdrawn at regular intervals and replaced with an equal volume of pre-equilibrated fresh buffer to maintain sink conditions. The concentration of Pep-B in the releasing medium was determined using ultraviolet spectrophotometer (Shimadzu, Japan, UV2450).

The percent erosion test was performed using a previously reported method [26]. Briefly, samples of 300 μl of the hydrogels were added into glass bottles, followed by photopolymerization with UV light for 15 s. After gelation, the original weight of the hydrogel samples was measured as (W0). Subsequently, 2 mL of ddH_2O were gently laid over the surface of the hydrogels and incubated at 37 °C with continuous gentle shaking. The weight of remaining hydrogels (Wt) was measured at regular intervals after completely blotting off the buffer. The remaining weight percentage was then calculated using the following relation:

$$Weight\ remaining\ (\%) = \frac{W0 - Wt}{W0} \times 100.$$

2.8. Animal experiment

All animal experimental procedures were performed according to a protocol approved by the Medical Laboratory Animal Center of Zhejiang University. 20 male *Sprague Dawley* rats (10 week, 300-330 g) were used and randomly divided into four groups (5 rats/group): blank group (without any treatment), periodontitis group (experimental periodontitis with saline injection), CMSA group (experimental periodontitis with CMSA treatment) and CMSA/Pep-B group (experimental periodontitis with CMSA/Pep-B treatment).

The periodontitis was inflicted using silk ligatures as described previously [27,28]. Briefly, the rats were anesthetized, then 4–0 silk ligatures were tied around the neck of the bilateral maxillary first molars. Subsequently, formulations (10 μL) were administered locally into the palatal gingiva between the maxillary first molar (M1) and second molar (M2) on a weekly basis, and then polymerized under UV light for 15 s. After treated for two weeks, all animals were euthanized and the entire palates were collected for following assay.

2.8.1. Enzyme-linked immunosorbent assay (ELISA)

The contents of C-reactive protein (CRP), IL-6, IL-1β, and TNF-α were measured in the serum and gingival crevicular fluid of rats using specific ELISA kits (Shijiazhuang Ximo Technology Co., Ltd) in accordance with the manufacturer's instructions.

2.8.2. RT-PCR

The gingiva tissues of the rats surrounding the first molar were collected and analyzed for the mRNA expression of IL-1β, IL-6, tumor necrosis factor-α (TNF-α), and monocyte chemoattractant protein-1 (MCP-1). In addition, alveolar bone between M1 and M2 were collected, and the mRNA expression of ALP, COL I, OPN and osteocalcin (OCN) were detected using the protocol in Section 2.5. The primers sequences are listed in Table S2.

2.8.3. Micro-computed tomography (micro-CT) analysis of periodontal bone

All palate samples were evaluated for alveolar bone quality using the Micro-CT system (MILabs BV, Heideibergiaan 100, Utrecht, 80,490, Netherlands). The X-ray source was set as follows: 80 keV and 500 mA, resolution 12.9 μm, exposure time 1880 ms, and aluminum filter 0.5 mm-thick. To generate 3D images, scanning raw data were reconstructed using IMALYTICS Preclinical software. Sagittal sections were generated using CT-Analyzer software.The linear distance from the cementoenamel junction to the alveolar bone crest (CEJ-ABC), where a long distance from CEJ to ABC was apprehended as more bone loss. CEJ-ABC distance of maxillary 1st molar tooth (M1) and 2nd molar tooth (M2) was measured to evaluate bone erosion. Additionally, bone-related parameters including bone mineral density (BMD), bone volume/tissue volume (BV/TV), trabecular thickness (Tb.Th), and trabecular separation (Tb.Sp) were measured. The ROI of the bone-related parameters measurement was the bone area between M1 and M2 and the teeth were excluded.

2.8.4. Histology

For histological analysis, the samples were fixed with 4 % paraformaldehyde, decalcified with ethylenediaminetetraacetic acid, embedded in paraffin, and cut into 5 μm sections in the midsagittal plane of the first molar. Hematoxylin & eosin (HE) and Masson's trichrome staining were used to stain the tissue sections. For immumohistochemical staining, after sealed by 3 % hydrogen peroxide, the slices were incubated with anti-IL-1β (1800) and anti-IL6 (1500) overnight. After that, the samples were incubated with secondary antibodies for 50 min, followed by staining with hematoxylin and diaminobenzidine, and were visualized using a microscopic. A part of each tissue section was subjected to tartrate-resistant acid phosphatase (TRAP) staining, and the positive cells with red staining on the alveolar bone surface were observed with microscopic analysis. Osteoclasts on the alveolar bone edges were evaluated using a semi-quantitative scoring system where 0 was assigned as negative, 1 as a few osteoclasts lining <5 % of alveolar bone surface, 2 as some osteoclasts (5–25 %), and 3 as many osteoclasts (25–50 %) [27]. For the collagen content estimation in the gingival mucosa, the sections were submitted to the picrosirius-red method and analyzed under polarized light. Image J was used to calculate the collagen content as previously described [29].

2.8.5. Safety evaluation in vivo

Different organs, including the heart, spleen, liver, and kidneys, were surgically excised from animals following euthanasia. These organs were immobilized in 4 % paraformaldehyde, embedded in paraffin sectioned into 5 μm and stained with HE. Finally, representative images were collected using a light microscope. Hematology and biochemical assays were conducted by collecting rat blood to assess the biocompatibility and in vivo toxicity of hydrogel. Blood biochemical parameters (including alkaline phosphatase, albumin, aspartate amino transferase, creatinine, total protein and urea) were analyzed using an automatic

biochemical analyzer (Wuhan service biotechnology Co. Ltd., China).

2.9. Statistical analysis

All data are presented as means ± standard deviations. Continuous outcomes among more than two groups were compared using one-way analysis of variance (ANOVA) using GraphPad Prism (version 7.0). The *p* value lower than 0.05 was considered as statistical significance.

3. Results

3.1. Character of Pep-B

The synthetic Pep-B was prepared by F-moc-based chemical solid phase synthesis from 15 amino acids (ACPIFTKIQGTCYRG) and the molecular structure of Pep-B was showed in Fig. S1. CD analysis showed that the secondary protein structure in Pep-B contained 8.20 % α-helix, 20.60 % β-sheet, 24.40 % β-turn and 46.80 % unordered structure (Fig. S2A, B). The bands at 1240 cm^{-1}, 1340 cm^{-1}, 1430 cm^{-1} and 1666 cm^{-1} in the Raman spectrum were assigned to a coil structure, an α-helical conformation, the CH2CH3 deformation and a β-strand structure (Fig. S2C). The result of mass spectrometry showed that molecular weight of Pep-B was 1658 Da (Fig. S2D), which was consistent with the designed peptide sequence. Pep-B chromatogram was measured at 214 nm absorption and the result showed that the purity of Pep-B was about 97 % (Fig. S2E).

3.2. Pep-B ameliorates LPS-induced cytotoxicity and oxidative stress

Stem cells play an important role in inflammation-induced damage repair, where LPS stimulation was reported to suppress stem cell activity [30]. First, phenotype of PDLSCs was identified by flow cytometry and results showed that PDLSCs were positive to MSC-specific surface markers CD29, CD90 and CD105, while negative to the hematopoietic cell antigens CD45, CD34 and microphage cell antigen CD11b (Fig. S3). Then, the effect of Pep-B in LPS-stimulated PDLSCs was explored as Fig. 1A. CCK8 result approved that LPS decreased the proliferation ability of PDLSCs, which was alleviated by applying an appropriate concentration of Pep-B (Fig. 1B). Stimulation with LPS resulted in a significant increase in ROS response, LDH release, and NO production relative to that in the unstimulated control group, while Pep-B treatment decreased ROS production (Fig. 1C, D), LDH release (Fig. 1E), and NO production (Fig. 1F) in LPS-stimulated PDLSCs. These results revealed that Pep-B could protect cells from LPS-induced cytotoxicity and played a vital role in mitigating LPS-induced oxidative stress.

3.3. Pep-B ameliorates LPS-induced inflammation and promotes the osteogenic differentiation of LPS-induced PDLSCs

PDLSCs are undifferentiated mesenchymal stem cells (MSCs) with multidirectional differentiation potential and self-renewal ability that can form cementum and periodontal ligament and maintain dynamic periodontal balance, and have broad prospects in periodontitis treatment [31,32]. However, it has been reported that these characteristics of PDLSCs tend to decrease to some extent under an inflammatory environment [33,34], which makes it imperative to improve these characteristics of PDL-SCs to provide an alternative treatment modality for periodontitis.

When PDLSCs were stimulated with 1 μg/mL LPS, the mRNA levels of pro-inflammatory genes (IL-1β, MCP-1, IL-6 and TNF-α) were significantly increased, which were markedly inhibited following Pep-B treatment (Fig. 1G).

Next, the effect of Pep-B on the osteogenic differentiation of PDLSCs under inflammatory conditions was explored as Fig. 2A. The ALP activity analysis results showed that ALP activity was suppressed in the LPS-induced inflammatory environment, which was significantly ameliorated following treatment with Pep-B compared to LPS group (Fig. 2B, D). Similarly, alizarin red staining results indicated that the mineralized areas were significantly decreased in the LPS group, while higher staining intensities were observed following applying the Pep-B treatment (Fig. 2C, E). In addition, RT-PCR results showed that the mRNA levels of osteogenic genes (ALP, COL I, BMP2, and OPN) in LPS-stimulated PDLSCs were inhibited compared to the control group, while Pep-B treatment significantly ameliorated this phenomenon on 7 and 14 days (Fig. 2F). These findings indicate that Pep-B holds potential to repair the osteogenic differentiation ability of PDLSCs under inflammatory conditions.

3.4. Characters of CSMA/Pep-B hydrogel

The schematic diagram of CMSA/Pep-B preparation was showed in Fig. 3A. CMSA/Pep-B hydrogel was in liquid state at room temperature, but transitioned to hydrogel under UV light for 15 s, indicating CMSA/Pep-B hydrogel had good photopolymerization ability (Fig. 3B). Moreover, CMSA/Pep-B hydrogel could be facilely transferred into a syringe and squeezed out from the needle which indicated CMSA/Pep-B hydrogel had good injectability (Fig. 3C). The representative SEM images revealed the hydrogels consisted of the loose and crosslinked network, and formed a highly porous 3D structure, which is deemed favorable to sustain the drug release, facilitate entry of cells, and exchange of nutrients/wastes (Fig. 3D, E). Rheological analysis of CMSA/Pep-B showed that there was a crossover point between G' and G", indicating that a sol-gel phase transition occurred (Fig. 3F). Drug release assay result showed that Pep-B was gradually released and almost completely released within 7 days (Fig. 3G). Degradation assay results showed that hydrogel degradation increased as incubation time increased, and hydrogels were almost completely degraded at day 7 (Fig. 3H). These results demonstrated the successful formulation of CMSA/Pep-B hydrogel and could sustain the Pep-B release to maintain sufficient concentration in the periodontal pocket.

3.5. CMSA/Pep-B hydrogel improves clinical indicators and inhibits the inflammatory response of periodontitis in vivo

During the development of periodontitis, several inflammatory immune responses occur, along with a substantial release of various pro-inflammatory cytokines in periodontal tissue. In this study, immunohistochemical staining, ELISA and RT-PCR were performed to explore the anti-inflammatory potential of CMSA/Pep-B in vivo, as shown in the schematic sketch (Fig. 4A). Immunohistochemical staining results indicated that the expression levels of IL-1β and IL-6 were significantly higher in the periodontitis group than in the blank group, suggesting the successful establishment of the periodontitis model; when compared to periodontitis group, the IL-1β and IL-6 expression levels in CSMA and CMSA/Pep-B groups decreased, and the decreased expression in CMSA/Pep-B group was more significant and closer to that of the blank group (Fig. 4B, C). Moreover, the serum and gingival crevicular fluid pro-inflammatory cytokines (CRP, IL-1β, IL-6, and TNF-α) levels in the periodontitis group were significantly higher than in other groups and were significantly decreased in CMSA/Pep-B group (Figs. 4D, S4). Consistent with ELISA results, RT-PCR results showed that the pro-inflammatory genes (IL-1β, IL-6, MCP-1 and TNF-α) expressions in the gingiva of the periodontitis group were significantly higher than blank group; slightly decreased in CSMA group, while markedly decreased in CMSA/Pep-B group (Fig. 4E). These findings demonstrated that CMSA/Pep-B hydrogel could significantly relieve inflammation response of periodontitis.

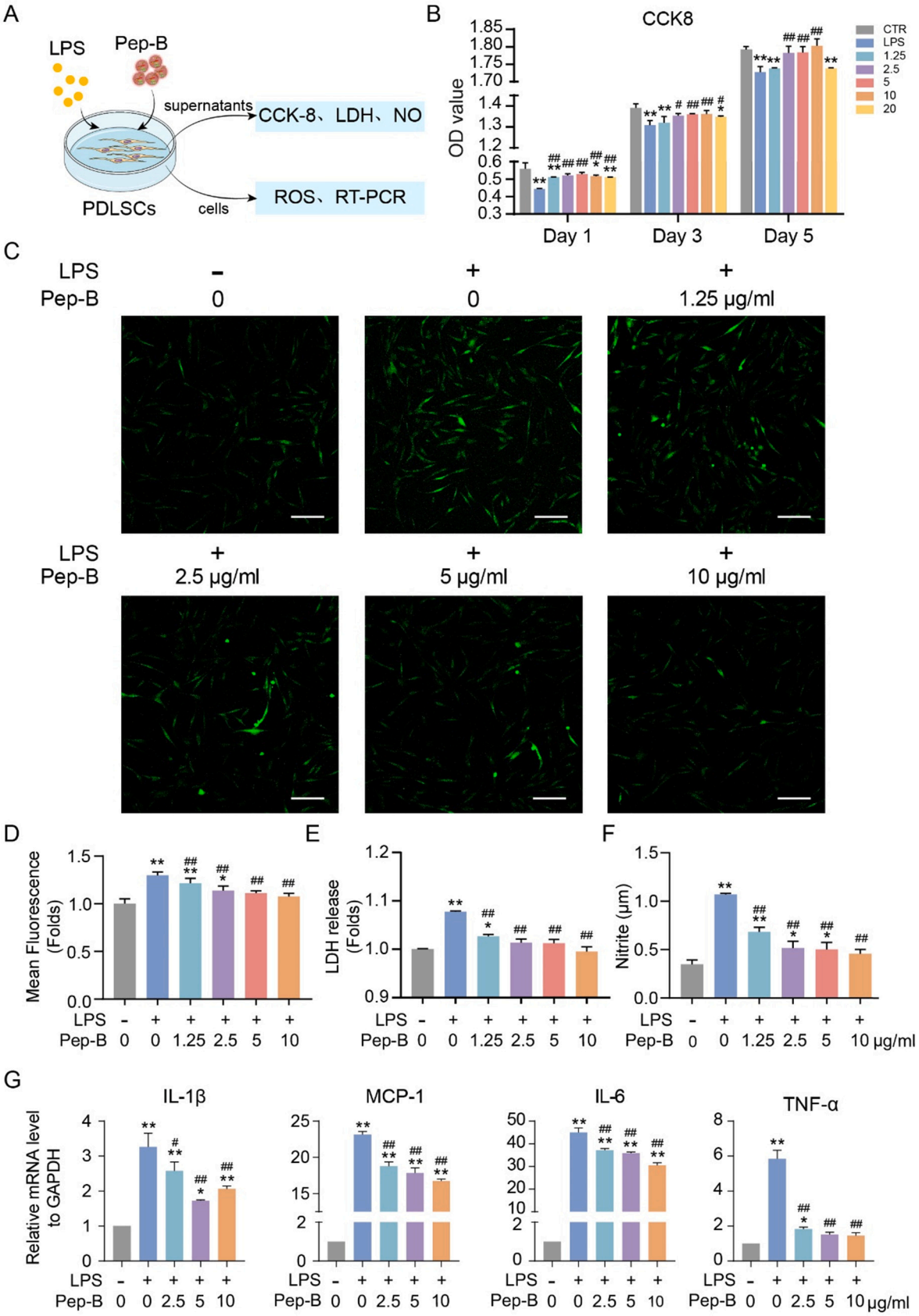

Fig. 1. Pep-B ameliorated LPS-induced cytotoxicity, oxidative stress and inflammation. (A) The sketch of experimental methods in vitro. (B) CCK-8 assay to detect the effect of Pep-B on LPS-induced PDLSCs. (C) Intracellular ROS level in PDLSCs. Scar bars are 50 μm. (D) Mean fluorescence of the intracellular ROS in PDLSCs. (E) The LDH release in PDLSCs. (F) NO production in PDLSCs. (G) RT-PCR assay to analyze the expression of proinflammatory genes in PDLSCs. $^{*}P < 0.05$, $^{**}P < 0.01$ compared with control group. $\#P < 0.05$, $\#\#P < 0.01$ compared with LPS group. Data are presented as means ± standard deviations, $n = 3$.

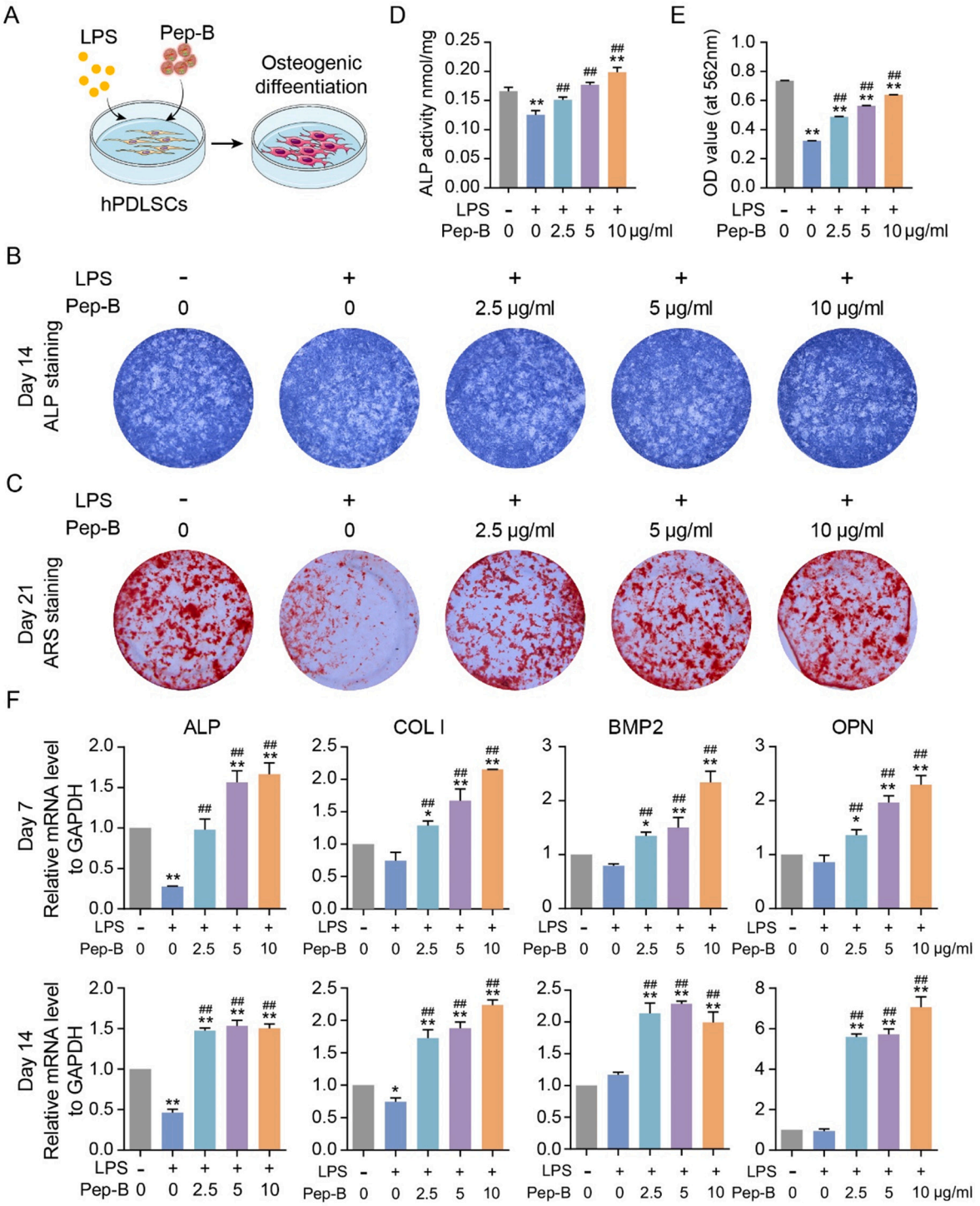

Fig. 2. Effects of Pep-B on the osteogenic differentiation in LPS-stimulated PLDSCs. (A) Schematic diagram of the cell processing method. (B) ALP staining at day 14. (C) ARS staining at day 21. (D) ALP activity at day 14. (E) Mineralization nodules quantification at day 21. (F) RT-PCR analysis of the mRNA expression of osteogenic-related genes at day 7 and 14. *P < 0.05, **P < 0.01 compared with control group. #P < 0.05, ##P < 0.01 compared with LPS group. Data are presented as means ± standard deviations, n = 3.

3.6. CMSA/Pep-B hydrogel inhibits periodontal tissue destruction of periodontitis in vivo

Periodontitis can destroy periodontal tissue, including alveolar bone, and ligament, etc. Therefore, an in vivo study was conducted to further confirm the intervention or protective effect of CMSA/Pep-B hydrogel on periodontal tissues of periodontitis. Periodontitis model in SD rats induced by ligature wire surrounding the maxillary first molar was showed in Fig. 5A. 3D reconstruction of maxillary alveolar showed that there was no substantial resorption of alveolar bone around tooth root in the blank group while substantial alveolar bone loss and root exposure were observed in the periodontitis group. Compared with the periodontitis group, CMSA and CMSA/Pep-B groups showed higher alveolar bone content, and the alveolar bone content in the CMSA/Pep-B group was closer to that in the blank group. The 2D images further confirmed this trend (Fig. 5B). In addition, CEJ-ABC distance was measured to

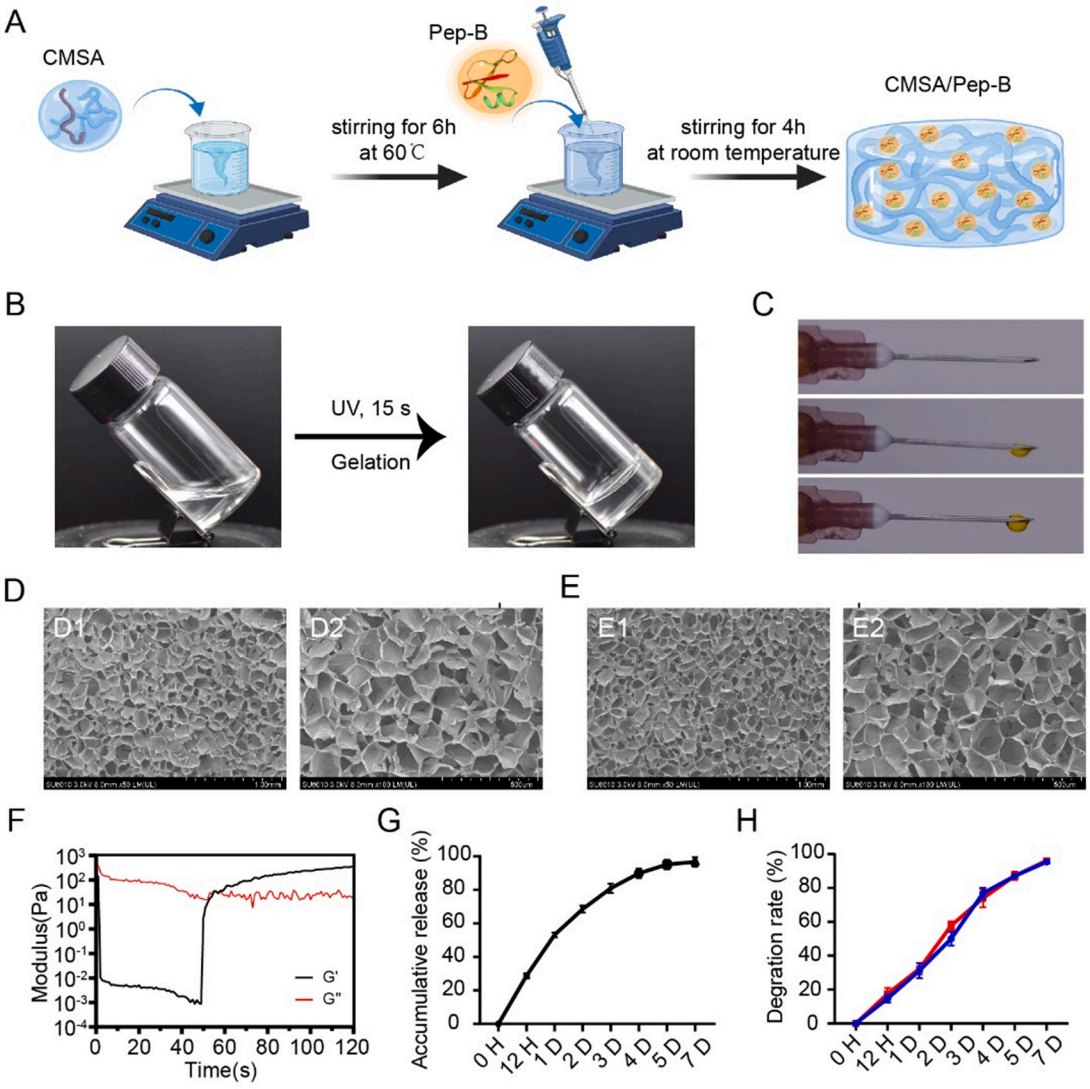

Fig. 3. Characters of CMSA/Pep-B hydrogel. (A) The schematic diagram of CMSA/Pep-B preparation. (B) The photopolymerizable ability of CSMA/Pep-B hydrogel. (C) The injection ability of CSMA/Pep-B hydrogel. (D) Representative SEM images of CMSA hydrogel. (E) Representative SEM images of CMSA/Pep-B hydrogel. D1, E1: Bar = 1 mm; D2, E2: Bar = 500 μm. (F) Rheological testing of CMSA/Pep-B hydrogel. (G) The release of Pep-B from CMSA/Pep-B hydrogel. (H) The degradation rate of CMSA and CMSA/Pep-B hydrogel.

evaluate the vertical bone loss, where the results showed that compared to periodontitis group, the CEJ-ABC distance in both CMSA and CMSA/Pep-B groups was smaller, but was close to the blank group in the CMSA/Pep-B group (Fig. 5C, D). The BMD, BV/TV, Tb.Th, and Tb.Sp are common bone mass change indices, where a high BMD, BV/TV, and Tb.Th values indicate high bone mass; the smaller Tb.Sp indicates a higher bone density. The results showed that the BMD, BV/TV, and Tb.Th in the CMSA/Pep-B group were significantly higher than the periodontitis and CMSA groups and was lower than the blank group. Similarly, Tb.Sp in the CMSA/Pep-B group was significantly lower than the periodontitis and CMSA groups and was higher than the blank group (Fig. 5E). The RT-PCR results showed that the osteogenic genes (ALP, COL I, OCN, and OPN) expressions in the alveolar bone between M1 and M2 were significantly decreased in the periodontitis group compared with the blank group, which was markedly ameliorated following the application of CMSA/Pep-B hydrogel (Fig. 5F).

The HE and Masson's trichrome staining results (as shown in Fig. 6A) revealed that the blank group showed no significant alveolar bone resorption, while the alveolar bone height was markedly decreased in the periodontitis group, which is a characteristic periodontitis symptom. Compared with that in the periodontitis group, the alveolar bone was repaired in the CMSA and CMSA/Pep-B groups, and the alveolar bone height in the CMSA/Pep-B group was obviously higher than that in the CMSA group. The Masson's trichrome staining further showed that most of the repaired alveolar bone in the CMSA/Pep-B group was mature bone tissue (Fig. 6B). The picrosirius-red stained sections of gingival mucosa in blank group under polarized light showed birefringent bundles of collagen fibers. In contrast, periodontitis group specimens exhibited weak birefringence, where the amount of birefringent material was significantly reduced compared to the blank group, while application of CMSA/Pep-B resulted in a significant increase in the birefringent content in the gingival mucosa (Fig. 6C, E). Moreover, TRAP staining visually showed that CMSA/Pep-B treatment practically decreased osteoclasts in the alveolar bone in periodontitis rats (Fig. 6D, G). These results further cemented the suitability of CMSA/Pep-B hydrogels in treating periodontitis.

The hematological and serum biochemical analysis results showed no pathological changes (Fig. S5). Furthermore, the pathological analysis showed no pathologic changes in the heart, spleen, liver, and kidney following CMSA/Pep-B application in rats, compared to the blank group (Fig. S6).

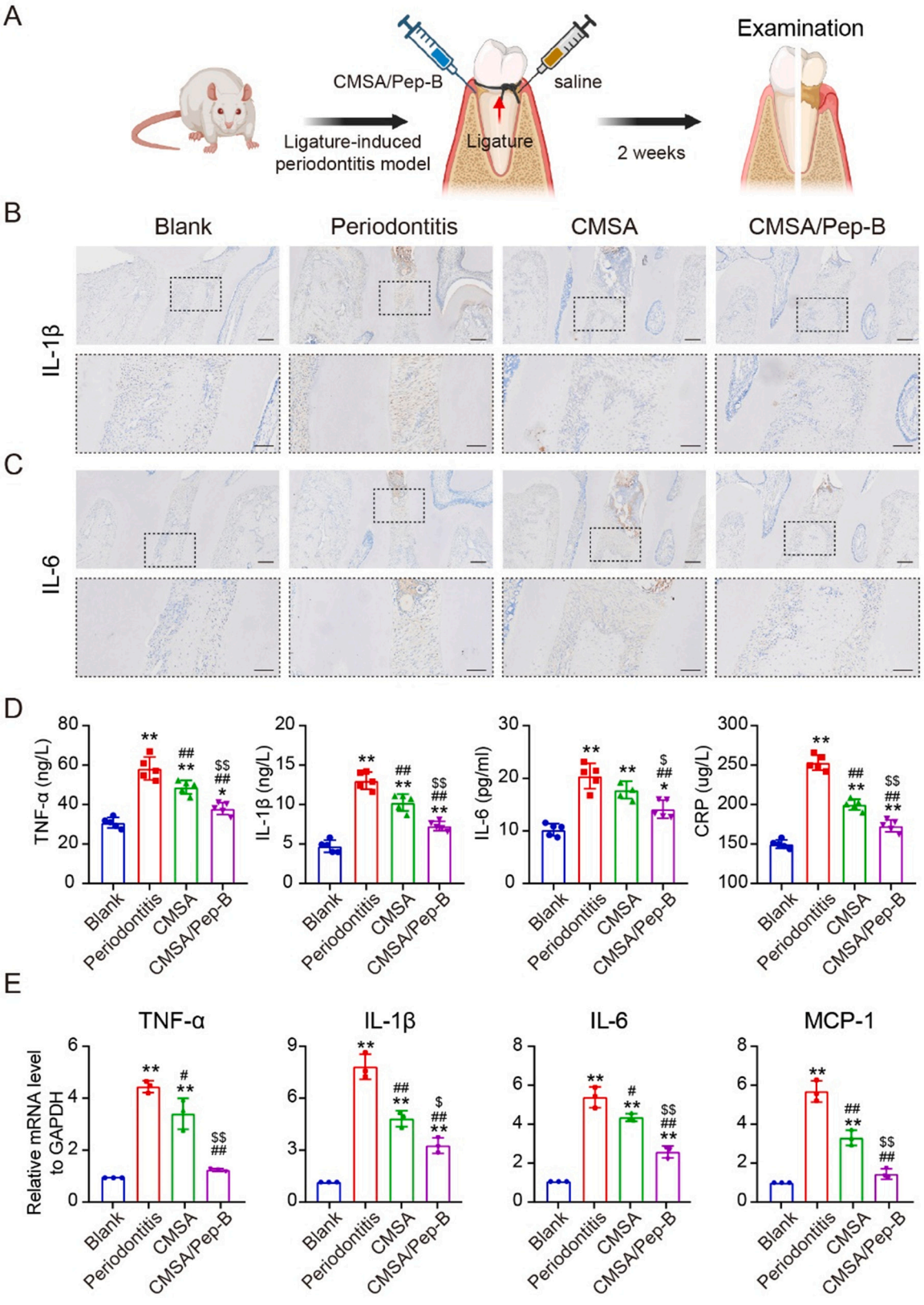

Fig. 4. CMSA/Pep-B hydrogel significantly reduced the inflammation of periodontitis in vivo. (A) Schematic diagram of the rat periodontitis experiment. (B) The immunohistochemical staining images of IL-1β of maxillary alveolar bone (Bar = 200 μm), the black borders show partial magnified images (Bar = 100 μm). (C) The immunohistochemical images of IL-6 of maxillary alveolar bone (Bar = 200 μm), the black borders show partial magnified images (Bar = 100 μm). (D) ELISA for TNF-α, IL-1β, IL-6 and CRP in gingival crevicular fluid, $n = 5$. (E) The mRNA expression of proinflammation genes in gingiva, n = 3. *P < 0.05, **P < 0.01 compared with blank group. #P < 0.05, ##P < 0.01 compared with periodontitis group. $P < 0.05, $$P < 0.05 compared with CMSA group. Data are presented as means ± standard deviations.

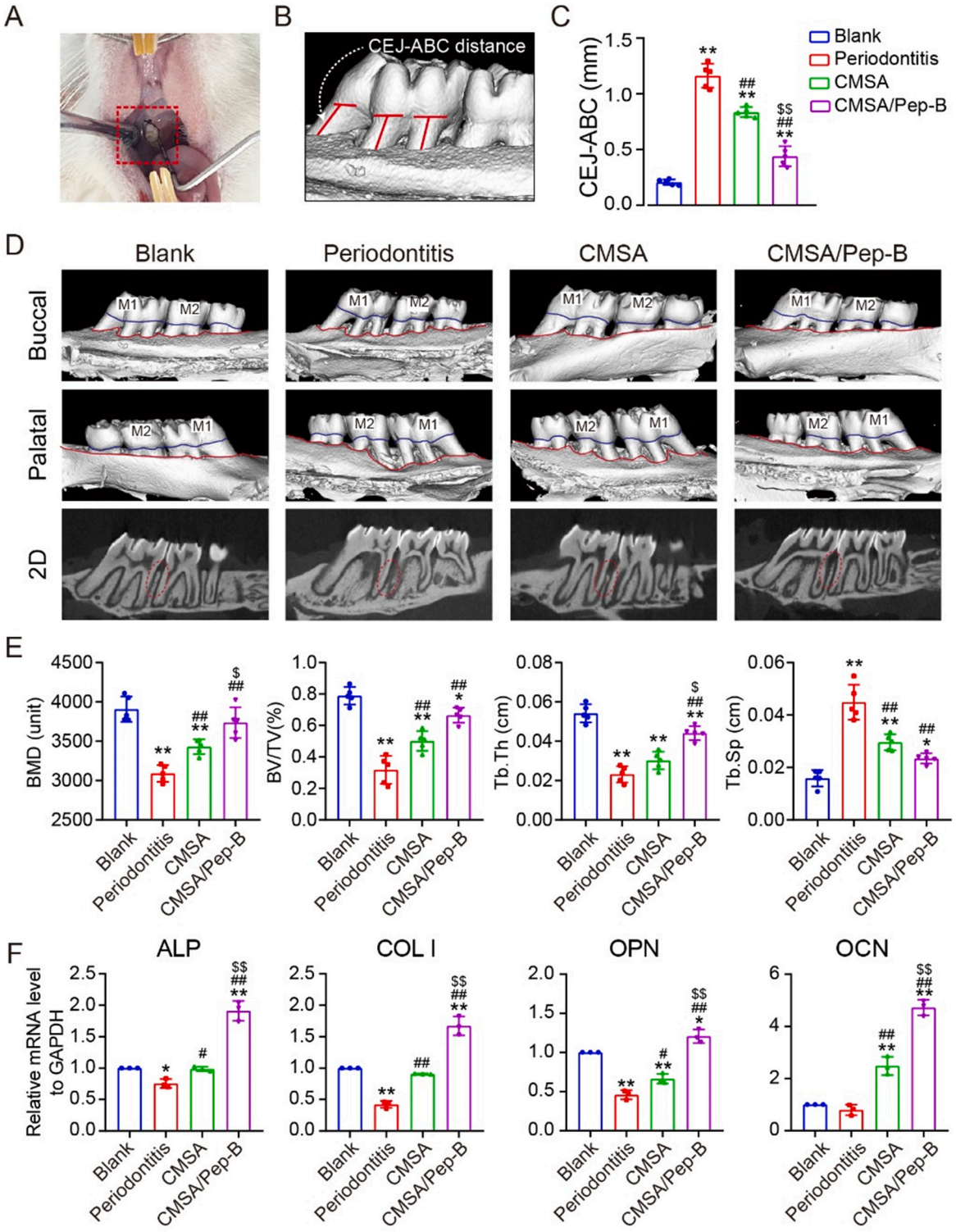

Fig. 5. CMSA/Pep-B hydrogel significantly inhibited alveolar bone loss in rat ligature-induced periodontitis. (A) A photograph of periodontitis model in SD rats induced by ligature wire surrounding the maxillary first molar. (B) The micro-CT 3D reconstruction images of maxillary alveolar bone. (C) A scheme of the vertical distance between CEJ and ABC. (D) Measurement of the linear distance between CEJ and ABC, n = 5. (E) Quantitative analysis of the micro-CT results of BMD, BV/TV, Tb.Th, and Tb.Sp, n = 5. (F) The mRNA expression of osteogenic-related genes of the alveolar bone between M1 and M2, n = 3. *P < 0.05, **P < 0.01 compared with blank group. #P < 0.05, ##P < 0.01 compared with periodontitis group. $P < 0.05, $$P < 0.05 compared with CMSA group. M1 = first maxillary molar; M2 = second maxillary molar. Data are presented as means ± standard deviations.

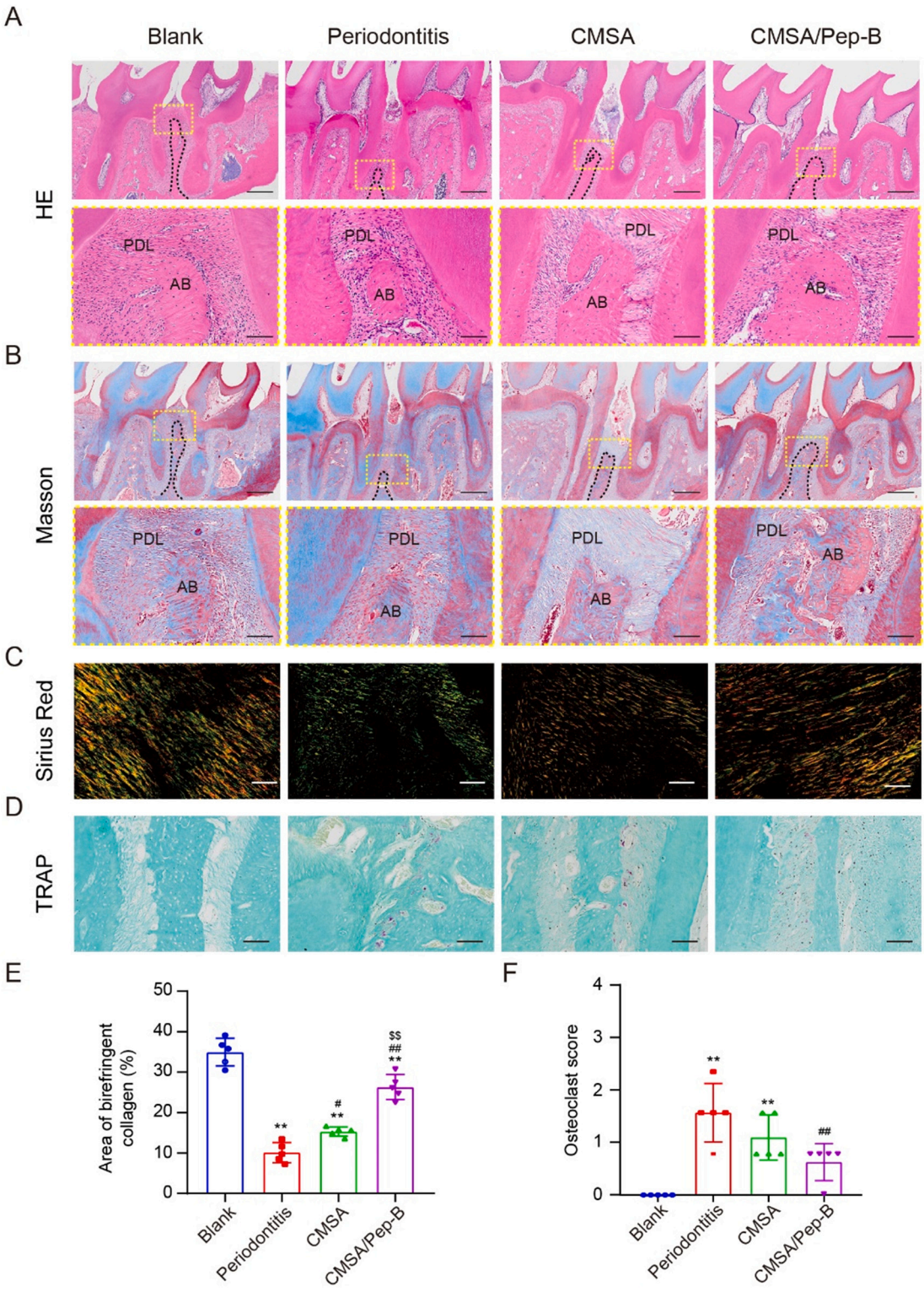

Fig. 6. CMSA/Pep-B hydrogel obviously inhibited the destroy of periodontal tissue from periodontitis in vivo. (A) The images of HE staining of maxillary alveolar bone (Bar = 500 μm), the yellow borders show partial magnified images (Bar = 100 μm). (B) The images of Masson's trichrome staining of maxillary alveolar bone (Bar = 500 μm), the yellow borders show partial magnified images (Bar = 100 μm). AB = alveolar bone; PDL = periodontal ligament. The area of black dotted line represents the alveolar bone. (C) The picrosirius-red stained sections of gingival mucosa under polarized light in different groups (Bar = 50 μm). (D) TRAP staining images in different groups (Bar = 100 μm). (E) The amount of birefringent collagen (%) in the gingival mucosa of different groups. (F) Semi-quantitative assessment of osteoclasts. *P < 0.05, **P < 0.01 compared with blank group. #P < 0.05, ##P < 0.01 compared with periodontitis group. $P < 0.05, $$P < 0.05 compared with CMSA group. M1 = first maxillary molar; M2 = second maxillary molar. Data are presented as means ± standard deviations, n = 5. (For interpretation of the references to color in this figure legend, the reader is referred to the web version of this article.)

4. Discussion

Periodontitis affects most of the population and is considered an important public health problem [1,35]. It is an inflammatory disease destroying periodontal tissue, including evident alveolar bone loss [2]. Currently, conventional antibiotics primarily manage periodontitis to control inflammation, ameliorate inflammation-induced damage, and reduce inflammatory alveolar bone loss. However, traditional antibiotics treatment has limited effectiveness in inhibiting periodontitis [36], and are prone to bacterial resistance and imbalanced oral flora [37,38]. As a functional fragment of human defensin β1, Pep-B is a natural antibiotic with many advantages, including no immunogenicity, high safety profile, and difficulty for pathogenic microorganisms to develop resistance. This project used Pep-B as a potential anti-inflammatory drug and developed it into an injectable photocurable chitosan hydrogel as a carrier. CMSA/Pep-B hydrogel can be minimally invasively injected into the periodontal pocket and release Pep-B sustainedly, with added merits of good therapeutic efficacy, high biosafety, and no effect on oral flora. Therefore, CMSA/Pep-B hydrogel is an ideal drug for periodontitis treatment to inhibit inflammation, reduce damage to periodontal tissue, and promote periodontium regeneration.

PDLSCs are considered ideal seeding cells to achieve real periodontium regeneration in periodontal tissue engineering due to their multi-lineage differentiation potential [31,39]. However, the existence of an inflammatory microenvironment poses a significant challenge to periodontium regeneration, because the continuous release of inflammatory factors can not only aggravate periodontal tissue destruction, but also affect periodontal bone regeneration by impairing the osteogenic differentiation of PDLSCs [33,34]. Therefore, inflammation control is a pivotal factor for periodontal tissue regeneration. Hence, the effect of Pep-B on LPS-stimulated PDLSCs was evaluated, and the results showed that when PDLSCs were continuously stimulated by LPS, the inflammatory response of PDLSCs aggravated and their osteogenic differentiation potential and mineralization capacity diminished; while Pep-B treatment reduced LPS-induced inflammation and restored osteogenic differentiation ability of PDLSCs. Recent studies have indicated that human β-defensin family has high affinity to LPS in vitro and can directly bond to LPS, thus to inhibit inflammatory response and rescue osteogenic differentiation ability of stem cells [40,41]. Moreover, our previous research also proved that Pep-B can inhibit inflammation of LPS-induced human dental pulp stem cells and promote the recovery of their osteogenic/dentinogenic capacity [24]. Therefore, it is hypothesized that Pep-B could repair and up-regulate the osteogenic differentiation of LPS-stimulated PDLSCs by inhibiting the expression of inflammatory factors and provide an appropriate anti-inflammatory microenvironment for tissue regeneration, making Pep-B a potential drug to enhance periodontium regeneration in periodontitis.

Systemic medication fails to achieve a high blood drug concentration in the local area; hence, it is necessary to restrict drug action primarily at the intended site. Local delivery of Pep-B into the periodontal pocket via CMSA/Pep-B hydrogel will permit drug direct targeting of periodontal tissue, achieving high local concentrations along with minimizing systemic toxicities. CMSA/Pep-B hydrogels effect was evaluated in vivo in a periodontitis rat model. Studies have proved that there are many inflammatory factors in periodontium of periodontitis which will lead to bone absorption and make the growth factors lose activity, thus weakening the regeneration and repair ability of periodontal tissue [42]. Our results confirmed that the local tissue inflammation in periodontitis rats was severe; while the application of CMSA/Pep-B could significantly relieve the inflammation response of periodontitis, which was envisaged to significantly reduce damage to periodontal tissue and promote a favorable microenvironment for subsequent alveolar bone regeneration. The micro-CT and histological staining results further confirmed these speculations, where compared to the periodontitis group, the alveolar bone in CMSA/Pep-B group was less damaged and was close to the normal alveolar bone. In addition, the number of osteoclasts, inflammatory infiltration, and collagen destruction were notably reduced after CMSA/Pep-B treatment. Therefore, it is concluded that Pep-B can timely alleviate the inflammatory microenvironment, reduce bone loss and facilitate the subsequent regeneration of alveolar bone. Moreover, the injectable therapeutic application of CMSA/Pep-B hydrogel is not only convenient but can also help achieve rapid drug administration, ensure high patient comfort, and reduce patient visits. Thus, CMSA/Pep-B hydrogel can be used as novel bioactive material for periodontitis treatment.

5. Conclusion

In conclusion, Pep-B can alleviate inflammation and rescue the osteogenic differentiation of PDLSCs under inflammatory conditions. The Pep-B was successfully loaded into chitosan, formulated into an injectable photopolymerizable CMSA/Pep-B composite hydrogel, and applied to treat periodontitis. The CMSA/Pep-B hydrogel exhibited excellent fluidity, which can be easily converted into a gel following UV light irradiation, sustaining the Pep-B release for up to one week. Furthermore, in vivo experiments showed that the local application of CMSA/Pep-B hydrogel can decrease periodontal inflammation, reduce periodontium destruction, and promote periodontal tissue regeneration. Above all, CMSA/Pep-B hydrogel has a good application prospect in periodontitis treatment.

CRediT authorship contribution statement

Jue Shi and Zihe Hu designed the research. Zihe Hu and Yanyan Zhou performed most of the experiments and wrote the manuscript. Haiyan Wu, Minghao Zuo, Gaoying Hong, Mumian Chen and Weiying Lu assisted in some studies. Wenjing Jin reviewed the manuscript. Jue Shi and Zhijian Xie supervised all the studies and the writing of the manuscript.

Declaration of competing interest

The authors declare that they have no known competing financial interests or personal relationships that could have appeared to influence the work reported in this paper.

Data availability

Data will be made available on request.

Acknowledgments

This work was supported by National Natural Science Foundation of China (grant numbers: 81801024) and Key R & D project of Zhejiang Science and Technology Department (grant numbers: 2021C03059). We thank Jingyao Chen, Chao Bi and Xiaoli Hong from the Core Facilities, Zhejiang University School of Medicine for their technical support in immunohistochemistry, Raman spectroscopy and confocal microscopy. We thank Zhiwei Ge from Analysis Center of Agrobiology and Environmental Sciences for technical assistance in Mass Spectrometry. We thank Home for Researchers editorial team (www.home-for-researchers.com) for language editing service.

Ethical approval

Study approval was obtained from the Ethics Committee of Zhejiang Stomatology Hospital (approval number: 2018013) and the Medical Ethics Committee of Zhejiang University (approval number: ZJU20220482).

Appendix A. Supplementary data

Supplementary data to this article can be found online at https://doi.org/10.1016/j.ijbiomac.2023.126060.

References

[1] D.K. Khajuria, O.N. Patil, D. Karasik, R. Razdan, Development and evaluation of novel biodegradable chitosan based metformin intrapocket dental film for the management of periodontitis and alveolar bone loss in a rat model, Arch. Oral Biol. 85 (2018) 120–129.

[2] R.P. Darveau, Periodontitis: a polymicrobial disruption of host homeostasis, Nat. Rev. Microbiol. 8 (7) (2010) 481–490.

[3] G. Hajishengallis, Periodontitis: from microbial immune subversion to systemic inflammation, Nat. Rev. Immunol. 15 (1) (2015) 30–44.

[4] P.M. Preshaw, S.M. Bissett, Periodontitis and diabetes, Br. Dent. J. 227 (7) (2019) 577–584.

[5] N.A. Hickey, L. Shalamanova, K.A. Whitehead, N. Dempsey-Hibbert, C. van der Gast, R.L. Taylor, Exploring the putative interactions between chronic kidney disease and chronic periodontitis, Crit. Rev. Microbiol. 46 (1) (2020) 61–77.

[6] R.J. Genco, T.E. Van Dyke, Prevention: reducing the risk of CVD in patients with periodontitis, Nat. Rev. Cardiol. 7 (9) (2010) 479–480.

[7] S.E. Choi, C. Sima, A. Pandya, Impact of treating oral disease on preventing vascular diseases: a model-based cost-effectiveness analysis of periodontal treatment among patients with type 2 diabetes, Diabetes Care 43 (3) (2020) 563–571.

[8] A.N. Wilson, M.J. Schmid, D.B. Marx, R.A. Reinhardt, Bone turnover markers in serum and periodontal microenvironments, J. Periodontal Res. 38 (4) (2003) 355–361.

[9] R.C. MacLean, A. San Millan, The evolution of antibiotic resistance, Science 365 (6458) (2019) 1082–1083.

[10] K. Jepsen, S. Jepsen, Antibiotics/antimicrobials: systemic and local administration in the therapy of mild to moderately advanced periodontitis, Periodontol 2000 71 (1) (2016) 82–112.

[11] A. Nazli, D.L. He, D. Liao, M.Z.I. Khan, C. Huang, Y. He, Strategies and progresses for enhancing targeted antibiotic delivery, Adv. Drug Deliv. Rev. 189 (2022), 114502.

[12] Y. Wei, Y. Deng, S. Ma, M. Ran, Y. Jia, J. Meng, F. Han, J. Gou, T. Yin, H. He, Y. Wang, Y. Zhang, X. Tang, Local drug delivery systems as therapeutic strategies against periodontitis: a systematic review, J. Control. Release 333 (2021) 269–282.

[13] E. Russo, C. Villa, Poloxamer hhydrogels for biomedical applications, Pharmaceutics 11 (12) (2019).

[14] D. Steinberg, M. Friedman, Sustained-release delivery of antimicrobial drugs for the treatment of periodontal diseases: fantasy or already reality? Periodontol 2000 84 (1) (2020) 176–187.

[15] Y. Shen, H. Tang, X. Huang, R. Hang, X. Zhang, Y. Wang, X. Yao, DLP printing photocurable chitosan to build bio-constructs for tissue engineering, Carbohydr. Polym. 235 (2020), 115970.

[16] D.K. Khajuria, S.F. Zahra, R. Razdan, Effect of locally administered novel biodegradable chitosan based risedronate/zinc-hydroxyapatite intra-pocket dental film on alveolar bone density in rat model of periodontitis, J. Biomater. Sci. Polymer edition 29 (1) (2018) 74–91.

[17] J. Liu, Y. Xiao, X. Wang, L. Huang, Y. Chen, C. Bao, Glucose-sensitive delivery of metronidazole by using a photo-crosslinked chitosan hydrogel film to inhibit Porphyromonas gingivalis proliferation, Int. J. Biol. Macromol. 122 (2019) 19–28.

[18] M.C.G. Pellá, M.K. Lima-Tenório, E.T. Tenório-Neto, M.R. Guilherme, E.C. Muniz, A.F. Rubira, Chitosan-based hydrogels: from preparation to biomedical applications, Carbohydr. Polym. 196 (2018) 233–245.

[19] E.V. Valore, C.H. Park, A.J. Quayle, K.R. Wiles, P.B. McCray Jr., T. Ganz, Human beta-defensin-1: an antimicrobial peptide of urogenital tissues, J. Clin. Invest. 101 (8) (1998) 1633–1642.

[20] K.R. Soldati, F.A. Toledo, S.G. Aquino, C. Rossa Jr., D. Deng, D.L. Zandim-Barcelos, Smoking reduces cathelicidin LL-37 and human neutrophil peptide 1-3 levels in the gingival crevicular fluid of patients with periodontitis, J. Periodontol. 92 (4) (2021) 562–570.

[21] D. Yilmaz, F. Caglayan, E. Buber, E. Könönen, Y. Aksoy, U.K. Gursoy, G.N. Guncu, Gingival crevicular fluid levels of human beta-defensin-1 in type 2 diabetes mellitus and periodontitis, Clin. Oral Investig. 22 (5) (2018) 2135–2140.

[22] A. Makeudom, C. Supanchart, P. Montreekachon, S. Khongkhunthian, T. Sastraruji, J. Krisanaprakornkit, S. Krisanaprakornkit, The antimicrobial peptide, human β-defensin-1, potentiates in vitro osteoclastogenesis via activation of the p44/42 mitogen-activated protein kinases, Peptides 95 (2017) 33–39.

[23] R. Sharma, U.N. Saikia, S. Sharma, I. Verma, Activity of human beta defensin-1 and its motif against active and dormant mycobacterium tuberculosis, Appl. Microbiol. Biotechnol. 101 (19) (2017) 7239–7248.

[24] J. Shi, Z. Hu, Y. Zhou, M. Zuo, H. Wu, W. Jin, Z. Xie, Therapeutic potential of synthetic human β-defensin 1 short motif Pep-B on lipopolysaccharide-stimulated human dental pulp stem cells, Mediat. Inflamm. 2022 (2022) 6141967.

[25] N. Liu, M. Zhou, Q. Zhang, L. Yong, T. Zhang, T. Tian, Q. Ma, S. Lin, B. Zhu, X. Cai, Effect of substrate stiffness on proliferation and differentiation of periodontal ligament stem cells, Cell Prolif. 51 (5) (2018), e12478.

[26] M. Deshmukh, Y. Singh, S. Gunaseelan, D. Gao, S. Stein, P.J. Sinko, Biodegradable poly(ethylene glycol) hydrogels based on a self-elimination degradation mechanism, Biomaterials 31 (26) (2010) 6675–6684.

[27] Y. Almoshari, R. Ren, H. Zhang, Z. Jia, X. Wei, N. Chen, G. Li, S. Ryu, S.M. Lele, R. A. Reinhardt, D. Wang, GSK3 inhibitor-loaded osteotropic Pluronic hydrogel effectively mitigates periodontal tissue damage associated with experimental periodontitis, Biomaterials 261 (2020), 120293.

[28] R.Y. Huang, H.Y. Chang, S.M. Chih, T.V. Dyke, C.D. Cheng, C.E. Sung, P.W. Weng, Y.S. Shieh, W.C. Cheng, Silibinin alleviates inflammation-induced bone loss by modulating biological interaction between human gingival fibroblasts and monocytes, J. Periodontol. (2023).

[29] J.P. de Pizzol Júnior, E. Sasso-Cerri, P.S. Cerri, Matrix metalloproteinase-1 and acid phosphatase in the degradation of the lamina propria of eruptive pathway of rat molars, Cells 7 (11) (2018).

[30] L. Zhang, L. Cheng, Y. Cui, Z. Wu, L. Cai, L. Yang, M. Duan, D. Zhang, C. Zhou, J. Xie, The virulence factor GroEL directs the osteogenic and adipogenic differentiation of human periodontal ligament stem cells through the involvement of JNK/MAPK and NF-κB signaling, J. Periodontol. 92 (11) (2021) 103–115.

[31] B.M. Seo, M. Miura, S. Gronthos, P.M. Bartold, S. Batouli, J. Brahim, M. Young, P. G. Robey, C.Y. Wang, S. Shi, Investigation of multipotent postnatal stem cells from human periodontal ligament, Lancet 364 (9429) (2004) 149–155.

[32] M.Y.O. Misawa, K.G. Silvério Ruiz, F.H. Nociti Jr., M.L. Albiero, M.T. Saito, R. Nóbrega Stipp, A. Condino-Neto, M. Holzhausen, H. Palombo, C.C. Villar, Periodontal ligament-derived mesenchymal stem cells modulate neutrophil responses via paracrine mechanisms, J. Periodontol. 90 (7) (2019) 747–755.

[33] X. Chen, C. Hu, G. Wang, L. Li, X. Kong, Y. Ding, Y. Jin, Nuclear factor-κB modulates osteogenesis of periodontal ligament stem cells through competition with β-catenin signaling in inflammatory microenvironments, Cell Death Dis. 4 (2) (2013), e510.

[34] M. Zhou, S. Gao, X. Zhang, T. Zhang, T. Zhang, T. Tian, S. Li, Y. Lin, X. Cai, The protective effect of tetrahedral framework nucleic acids on periodontium under inflammatory conditions, Bioact. Mater. 6 (6) (2021) 1676–1688.

[35] N.J. Kassebaum, E. Bernabé, M. Dahiya, B. Bhandari, C.J. Murray, W. Marcenes, Global burden of severe periodontitis in 1990-2010: a systematic review and meta-regression, J. Dent. Res. 93 (11) (2014) 1045–1053.

[36] T.F. Mah, B. Pitts, B. Pellock, G.C. Walker, P.S. Stewart, G.A. O'Toole, A genetic basis for Pseudomonas aeruginosa biofilm antibiotic resistance, Nature 426 (6964) (2003) 306–310.

[37] N. Høiby, T. Bjarnsholt, M. Givskov, S. Molin, O. Ciofu, Antibiotic resistance of bacterial biofilms, Int. J. Antimicrob. Agents 35 (4) (2010) 322–332.

[38] P.S. Stewart, J.W. Costerton, Antibiotic resistance of bacteria in biofilms, Lancet 358 (9276) (2001) 135–138.

[39] X. Kong, Y. Liu, R. Ye, B. Zhu, Y. Zhu, X. Liu, C. Hu, H. Luo, Y. Zhang, Y. Ding, Y. Jin, GSK3β is a checkpoint for TNF-α-mediated impaired osteogenic differentiation of mesenchymal stem cells in inflammatory microenvironments, Biochim. Biophys. Acta 1830 (11) (2013) 5119–5129.

[40] Y. Zhai, Y. Wang, N. Rao, J. Li, X. Li, T. Fang, Y. Zhao, L. Ge, Activation and biological properties of human β defensin 4 in stem cells derived from human exfoliated deciduous teeth, Front. Physiol. 10 (2019) 1304.

[41] H. Yu, J. Dong, Y. Gu, H. Liu, A. Xin, H. Shi, F. Sun, Y. Zhang, D. Lin, H. Diao, The novel human β-defensin 114 regulates lipopolysaccharide (LPS)-mediated inflammation and protects sperm from motility loss, J. Biol. Chem. 288 (17) (2013) 12270–12282.

[42] Q. Yan, Y. Li, N. Cheng, W. Sun, B. Shi, Effect of retinoic acid on the function of lipopolysaccharide-stimulated bone marrow stromal cells grown on titanium surfaces, Inflamm. Res. 64 (1) (2015) 63–70.